Differential cross sections for electron-impact excitation of the electronic states of N_2

M. J. Brunger and P. J. O. Teubner
Institute for Atomic Studies, School of Physical Sciences, The Flinders University of South Australia, Bedford Park, South Australia
(Received 13 April 1989)

Differential cross sections for the electron-impact excitation of the first ten electronic states of N_2 have been determined at five incident energies ranging from 15 to 50 eV. These differential cross sections were obtained for the scattering range 10°–90° by analyzing electron-energy-loss spectra in N_2 at a number of fixed scattering angles within that range. The present study represents a comprehensive remeasurement of the earlier work of Cartwright and co-workers [Phys. Rev. A **16**, 1013 (1977)] and was undertaken with a view to resolving certain anomalies which have been reported in the literature when the earlier cross-section set has been applied to model calculations of swarm parameters.

I. INTRODUCTION

The need for accurate electron-molecule collision cross sections to aid an understanding of fundamental and applied physical phenomena in the study of gaseous electronics, laser physics, plasma physics, and the physics of the upper atmosphere has been well documented.[1] A comprehensive review of experimental methods and data for electron scattering from molecules has been provided by Trajmar, Register, and Chutjian.[2] In particular, they collated and systematically quantified the then existing data for elastic, rotational, vibrational, and electronic excitation cross sections in N_2. Subsequently, additional work on a few experimental studies of electronic excitation in N_2 has been reported. This work includes the differential and integral cross-section measurements of Zetner and Trajmar,[3] who extended the earlier work of Cartwright and co-workers[4,5] to lower energies, the integral cross-section measurements for the $X\,^1\Sigma_g^+ \rightarrow a\,^1\Pi_g$ electron-impact excitation as reported by Ajello and Shemansky[6] and Mason and Newell[7] and a recent, near-threshold, integral cross section for the excitation of the $E\,^3\Sigma_g^+$ electronic state as measured by Brunger, Teubner, and Buckman.[8]

A detailed review of the status of the theory of electron-impact excitation of molecules was provided by Trajmar and Cartwright.[9] As an adjunct to this more recent theoretical studies of molecules are well summarized in two articles by Collins and Schneider.[10,11] Here an overview of the formalism for electron-molecule scattering is given and the approximations commonly used to make the solution more tractable. While it is clear from these articles[10,11] that there has been a large amount of activity since the earlier review[9] it is apparent that very little of it has been directed to calculating cross sections for excitation of the electronic states of N_2. Indeed, until recently the only calculations available in the literature were those which utilized the Born approximation with the Ochkur[12] and Rudge[13] scheme for treating the electron exchange-scattering amplitudes. These calculations have been performed by Rozsnyai,[14] Cartwright,[15] and Chung and Lin,[16] and while these authors do not calculate cross sections for excitation of exactly the same set of electronic states, the only practical difference between them was in their respective choice of basis states for the calculations. More recently, Huo *et al.*[17] have applied a Schwinger multichannel formulation to calculate cross sections for excitation of the $B\,^3\Pi_g$, $A\,^3\Sigma_u^+$, $C\,^3\Pi_u$, $a\,^1\Pi_g$, $a'\,^1\Sigma_u^-$ and $w\,^1\Delta_u$ electronic states from the ground-electronic state ($X\,^1\Sigma_g^+$) while Gillan *et al.*[18] have stated their intention to extend their R-matrix method to calculate cross sections for excitation of electronic states in N_2.

The present study repeats the pioneering differential cross-section experiments of Cartwright *et al.*[4] for excitation of electronic states in N_2 and was initiated to provide more experimental data to aid the development of theoretical models and in an attempt to resolve a controversy which has arisen because of discrepancies which exist between the published data of Cartwright *et al.*[5] and the cross-section sets used in Monte Carlo simulations of gas discharges. The genesis of these discrepancies appears to have originated in the work on Monte Carlo simulations of Townsend discharges in N_2 by Taniguichi, Tagashira, and Sakai,[19] who modified the then available cross-section data to obtain agreement with swarm parameters. This work was submitted for publication prior to the completion of the work of Cartwright and coworkers.[4,5] In response to the publication of this new data Tagashira, Taniguichi, and Sakai[20] updated the work of Taniguichi, Tagashira, and Sakai[19] and found that it was necessary to reduce the magnitude of the cross sections of Cartwright *et al.*,[5] describing excitation to the electronic states with thresholds below 12.25 eV, by 15% in order to obtain agreement with measurements of the experimental swarm parameters α_T, D_L, and W in an electric field.

Subsequently, Phelps and Pitchford[21,22] compiled a new set of cross-section data for N_2 which were compatible with a wide range of existing transport and coefficient

data as obtained in gaseous electronic experiments. This set disagreed with that of Tagashira, Taniguichi, and Sakai[20] and in part with the measurements of Cartwright *et al.*[5] on electronic transitions in N_2; for example, they[22] propose a large increase in the value of the $C\ ^3\Pi_u$ integral cross section (a factor of 2 increase at the peak) and a substantial change to the threshold behavior of the $E\ ^3\Sigma_g^+$ cross section.

Clearly this controversy can only be resolved by an independent remeasurement of the cross sections for the excitation by electron impact of the first ten electronic states in N_2. This paper details results of such a study. In Secs. II and III we describe the experimental apparatus and procedures, respectively, which were used to obtain the present data. The results are presented and discussed in Sec. IV.

II. EXPERIMENTAL APPARATUS

The electron monochromator which was used in the present experiments is shown schematically in Fig. 1. It consisted of two parts—a selector which produced a beam of electrons with an energy half-width of ~40 meV and an analyzer which analyzed the energy of the scattered electrons with a similar energy resolution. Both sections of the monochromator used hemispherical geometry for the dispersive stages.

The primary source of electrons was a tungsten hairpin cathode used in a standard triode configuration. The image produced by this source at GA1 was then focused by two three-aperture lenses (GL1 and GL2) at the entrance plane of the hemispherical selector. The overall magnification of these lenses was essentially unity and the electron filling factor in all the optics was kept as low as possible in order to minimize aberration and lens surface effects. The pencil half angle and the beam angle at the selector entrance were made small by the two defining apertures GA2 and GA3.

Special care was taken to shield all insulating surfaces from the electron beam. In addition, all surfaces exposed to the electron beam were manufactured from molybdenum. The operating potentials for the lens modules were derived from the calculations of Harting and Read.[23]

A detailed description of the principles of operation for the hemispherical selectors can be found in Read *et al.*[24] or Imhof, Adams, and King.[25] The design of the correction electrodes for fringing fields in the selector and analyzer was based on the material described by Brunt,

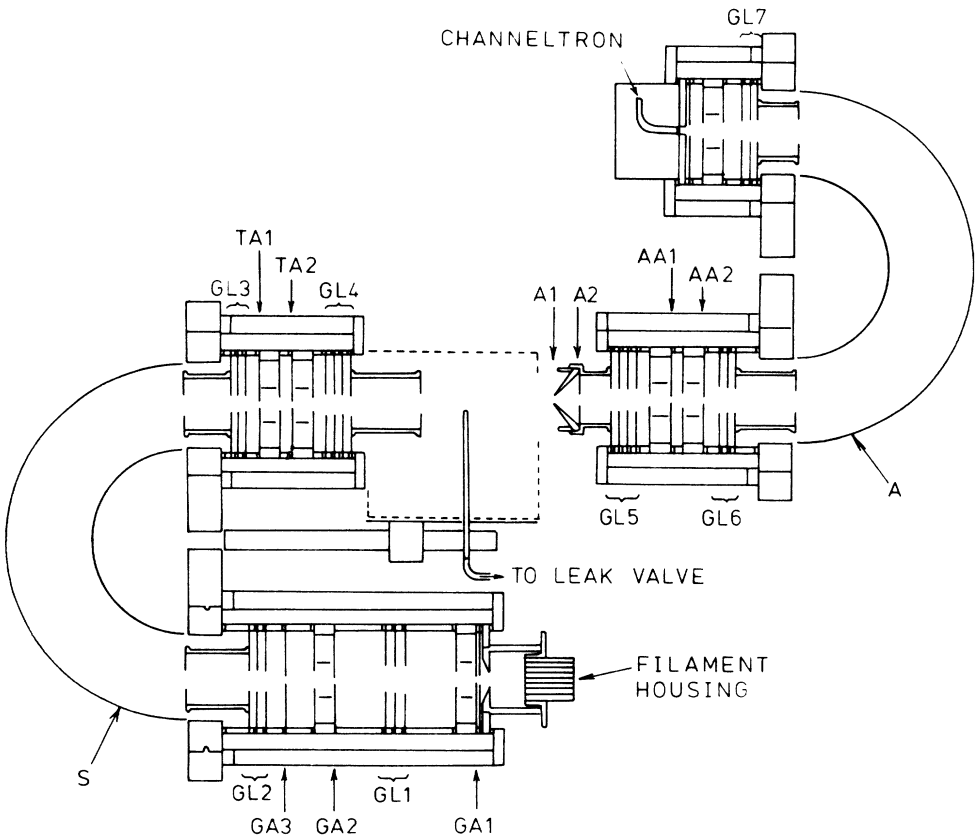

FIG. 1. Schematic diagram of the electron monochromator. *S* denotes the hemispherical selector, while *A* denotes the hemispherical analyzer.

Read, and King.[26] These electrodes were manufactured from 310 grade stainless steel and coated with molybdenum using a sputtering technique. The resulting electric field in the hemisphere focused the electron beam onto its exit plane with unit magnification.

The second lens module was used to transport the electron beam to the interaction region. It design was based on the design principles given by Brunt, Read, and King.[26] The lens GL4 was operated as a zoom lens in order to accommodate the range of final beam energies required in the experiments.

The angular field of view of the analyzer was defined by the entrance pupil A1 while the window A2 defined the diameter of the region of acceptance at the interaction region. The diameter of both A1 and A2 was 1 mm and A2 was placed at the principal focus of GL5. The angular field of view of the analyzer was approximately 12° and the region of acceptance at the interaction region was 3.5 mm in diameter.

A conventional design was used for the electron optics of lens module 3 which transported the scattered electrons from the interaction region to the entrance plane of the hemispherical analyzer. This module was designed so that an exchange of window and pupil occurred in order to ensure that the beam angle at the entrance plane was small. This was achieved by requiring the defining aperture AA2 to be at the image distance of GL5 while AA1 was at the object distance of GL6.

It was necessary to maintain the image position of GL5 at AA2 for a wide variety of kinetic energies of the scattered electrons. Thus GL5 was chosen to be a zoom lens containing four individual elements of which three, at any given time, had independent potentials applied to them. In addition, provision was made to apply a linear voltage ramp to the middle element of GL5 so that the transmission of the module was independent of the kinetic energy of the scattered electrons. We have discussed this feature of the monochromator in detail elsewhere (Brunger *et al.*[27]). Briefly, a technique which was first suggested by Pichou *et al.*[28] was used to demonstrate that the transmission of the scattered electrons from helium was constant to better than 5% over a wide range of residual energies. The results of such an experiment are shown in Fig. 2.

After energy analysis, the scattered electrons were transported by lens GL7 to a channel electron multiplier. The mean energy of electrons in the analyzer was ~1 eV thus GL7 was designed with a high accelerating ratio to optimize the efficiency of the channel electron multiplier.

Output pulses from the detected electrons were amplified and recorded in a multichannel analyzer operating in the multichannel scaling mode (MCS). The voltage ramp which was applied to the analyzer earth was synchronized with the channel advance on the multichannel scaler. It was established that the x axis of the MCS was linearly related to the ramp voltage to better than 0.1%. The data could be transferred from the MCS to a mainframe computer where the data analysis, described in the next section, was performed.

The monochromator could be operated in either of two different modes. The "energy-loss" mode was used to record the spectra from which the electronic state differential cross sections were derived. In this mode the beam energy was held constant and the analyzer earth was ramped. Thus the analyzer was tuned to accept electrons which had lost a varying amount ΔE of their kinetic energy. The "impact energy" mode[29] was used to calibrate the beam energy in a manner which is described in Sec. III. Here the beam energy was varied linearly while the analyzer was tuned to transmit a particular energy-loss feature. In this mode allowance was made to supply a linear voltage ramp to the middle element of lens GL4B to compensate for possible energy-dependent variations in the incident current and beam profile.

III. EXPERIMENTAL PROCEDURE

The energy of electrons scattered from the molecular beam at a given scattering angle was analyzed for each incident energy by operating the analyzer in the energy-loss mode. A typical energy-loss spectrum which covers the energy-loss range W: 6 eV < W < 12.4 eV is shown in Fig. 3. The complex structure arises from the fact that

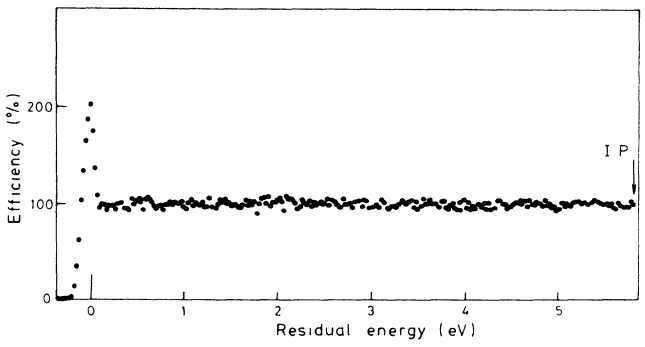

FIG. 2. Transmission efficiency of the analyzer. We have assumed that the percent efficiency at the ionization potential in helium is equal to 100%.

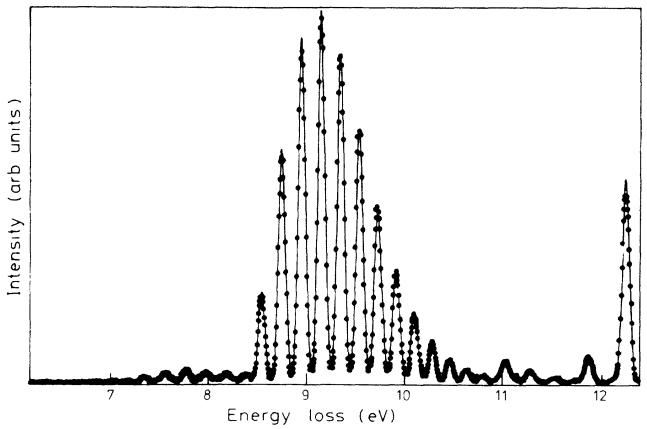

FIG. 3. Energy-loss spectrum in N_2. The electron scattering angle was 10° and the incident electron beam energy was 30 eV. The present data (●) and the fit to this data (——) are shown.

there are ten electronic transitions each with overlapping vibrational bands in this energy range. We note, however, that the $a''\,^1\Sigma_g^+$ state at an energy loss of 12.253 eV is quite well resolved. Thus we were able to use this state as a benchmark to provide ratios of the cross sections for the various electronic transitions to that for the a'' state. The deconvolution technique which was used as a basis for these ratios is described in the next section.

We define the ratio $R_{n'}$ as

$$R_{n'}=\frac{\mathcal{I}(n')}{\mathcal{I}(a''\,^1\Sigma_g^+)} \tag{1}$$

where n' denotes the electronic state of interest and is depicted schematically in Fig. 4.

The ratios $R_{n'}$ were determined from spectra taken at each scattering angle θ in the range $10°\leq\theta\leq 90°$. The 0° position was identified by either rotating the analyzer through the primary electron beam or from the symmetry of the scattered intensity about the true zero scattering angle. This procedure was repeated for each incident energy.

In a separate set of experiments the scattered intensity from the a'' state was compared to the elastically scattered intensity at each scattering angle for each incident energy. This ratio R_e is defined as

$$R_e=\frac{\mathcal{I}(a'')}{\mathcal{I}_{\rm el}}\,. \tag{2}$$

This ratio was measured by taking energy-loss spectra in the range $-0.4\ \text{eV}\leq W\leq 12.4\ \text{eV}$ and by recording the number of scattered electrons at the elastic peak energy loss and at 12.253 eV energy loss. After allowing for background contributions, the product $R_{n'}R_e$ then gave the ratio of the inelastically scattered signal to the elastically scattered signal for each electronic state. This procedure minimized the influence of systematic effects arising from long-term drifts in the electron and target beam densities. It also removed the influence of geometrical angle-dependent effects on the measurements.

Two contributions to this background were identified; that is, scattering from the residual gas in the chamber and primary beam interference. The latter effect was only significant at energies $E_0<20$ eV and scattering angles $\theta\leq 15°$ while the former was present at all angles. The influence of both these contributions together with the dark noise in the detector and stray electron counts was studied by turning the N_2 beam off and subtracting the appropriate number of events. In all cases the background constituted less than 2% to the detected signal. This reflected the low base pressure in the chamber ($\sim 1\times 10^{-8}$ torr). The background contribution to the inelastic signal was essentially set by stray electrons and dark noise. Allowance was made for these effects by appropriate "beam-off" measurements. In general, the maximum background contribution to the inelastic signal was less than 2%. The consistency of this background subtraction technique was tested by the fit in Eq. (5) where we invariably found $B=0$.

The product $R_{n'}R_e$ was converted to a differential cross section by using the appropriate differential cross sections for elastic scattering.

In the present study, experiments were conducted at incident electron beam energies of 15, 17.5, 20, 30, and 50 eV. The incident beam energy was calibrated against the known energy of the $2\,^2S$ resonance in helium by operating the monochromator in the "impact-energy" mode with the analyzer set to detect electrons which had been elastically scattered at 90° from helium target atoms.

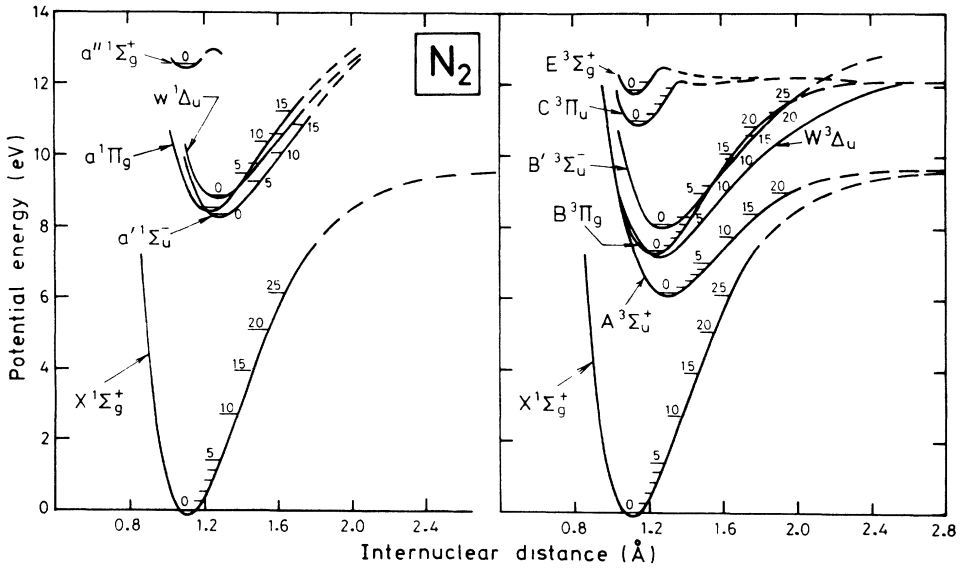

FIG. 4. Schematic diagram of the electronic states of N_2.

A. Data analysis

Each energy-loss spectrum was analyzed using a computer least-squares-fitting technique which was first described by Trajmar, Cartwright, and Williams.[30] Subsequently, Cartwright and co-workers[4,5] refined the technique in their N_2 studies. In this technique the separation energies of the electronic transitions are assumed known as are the Franck-Condon factors connecting each vibrational level of the excited electronic states with the lowest vibration level of the ground-electronic state. The fitting procedure then yields relative intensities for inelastic scattering from the various excited electronic states. These intensities when summed appropriately are proportional to the required differential cross section.

Following Trajmar, Cartwright, and Williams,[30] the rotationally averaged differential cross section for excitation of the vibrational level v' of electronic state n' at an incident energy E_0 and scattering angle of θ is denoted as $\sigma_{n'v'}(E_0,\theta)$. The scattered signal $S(E_0,\theta,W)$ at a particular angle θ and energy loss W for a given incident energy E_0 is

$$S(E_0,\theta,W)=I_0C(E_0,\theta)\rho\sum_{n'=0}^{N}\sum_{v'=0}^{M(n')}\sigma_{n'v'}(E_0,\theta)\times F(W_{n'v'}-W)\ , \tag{3}$$

where $C(E_0,\theta)$ is a constant at a given impact energy which incorporates the effective path-length correction and all instrumental efficiency factors, N is the total number of electronic transitions, $M(n')$ the number of vibrational bands within a given electronic state, I_0 the incident electron beam current, and ρ the target beam density. The function $F(W_{n'v'}-W)$ characterizes the energy resolution of the analyzer.

Equation (3) is further simplified by assuming the validity of the Born-Oppenheimer approximation. Thus the relative vibrational intensities are independent of the incident energy and scattering angle:

$$\sigma_{n'v'}(E_0,\theta)=\sigma_{n'}(E_0,\theta)q_{v'v''}\ . \tag{4}$$

Here $q_{v'v''}$ is the Franck-Condon factor and $\sigma_{n'}(E_0,\theta)$ is the differential cross section for a given electronic transition at the angle θ.

Substituting Eq. (4) into Eq. (3) gives

$$S(E_0,\theta,W)=\sum_{n'=0}^{N}X_{n'}(E_0,\theta)\sum_{v'=0}^{M(n')}q_{v'v''}F(W_{n'v'}-W)+B(E_0,\theta,W)\ , \tag{5}$$

where

$$X_{n'}(E_0,\theta,W)=I_0\rho C(E_0,\theta)\sigma_{n'}(E_0,\theta)\ . \tag{6}$$

The term $B(E_0,\theta,W)$ represents any background contribution to the measured signal. In the current study we followed the lead of Cartwright *et al.*[4] by representing the background in the form

$$B=\sum_{i=1}^{4}a_iW^{i-1}\ . \tag{7}$$

The form of the background, as given by Eq. (7), was found to be an excellent representation of that measured experimentally throughout the present study which reflects the excellent signal-to-noise ratio across the entire energy-loss range. The experimental resolution function $F(W_{n'v'}-W)$ was shown to be Gaussian in form so that

$$F(x)=\frac{1}{\Delta\sqrt{2\pi}}\exp\left[\frac{-x^2}{2\Delta^2}\right]\ , \tag{8}$$

where Δ is the full width at half maximum (FWHM) energy resolution and is a parameter to be determined in the fit.

The quantities $X_{n'}(E_0,\theta)$ and a_i are determined, for a given energy-loss spectrum, from Eqs. (5) and (7) by requiring that the difference between the measured and calculated spectrum be a minimum in a least-squares sense (Cartwright *et al.*[4]). The coefficients $X_{n'}(E_0,\theta)$, for a given spectrum, are proportional to the differential cross sections for excitation of the electronic states n'. The normalization procedure for making these coefficients absolute is discussed later in the paper.

The techniques described above assume a knowledge of the energy of each vibrational sublevel relative to the $v''=0$ vibrational sublevel of the $X\,^1\Sigma_g^+$ ground-electronic state and the corresponding Franck-Condon factors.

In the present work the majority of the Franck-Condon factors were obtained from the tables of Krupenie and Lohftus.[31] The Franck-Condon factors which were unavailable in Krupenie and Lohftus[31] were obtained from other sources. These include the work of Benesch *et al.*[32] and Cartwright.[15] Cartwright[15] has discussed the applicability of the Franck-Condon approximation for processes originating from the $v''=0$ ($X\,^1\Sigma_g^+$-state) level. He has shown that for this specific case, except near threshold, the Franck-Condon approximation is quite good and he has proposed that this result is due to the fact that the initial vibrational wave function is Gaussian in character and centered at the equilibrium separation distance R_e of the initial electronic state. Consequently, the major contribution to the excitation amplitude must occur at this same R_e and so the Franck-Condon approximation should be reasonably valid. Near threshold this is not necessarily the case. Thus Zetner and Trajmar[3] have introduced "flux-factor corrected" Franck-Condon factors in their recent studies in N_2. In the present study, however, we are always working at electron-impact energies greater than 2.5 eV above the excitation threshold of the electronic states which implies that the current Franck-Condon factors should be adequate in the present analysis (Trajmar[33]).

The energy levels of the various vibrational substates, for a given electronic state, were calculated from a set of spectroscopic data tables supplied by Wedding,[34] although we note that the energies of the $E\,^3\Sigma_g^+$ state $v'=0$ and 1 states were taken from Cartwright.[15]

A typical example of the application of the fitting pro-

cedure to a measured energy loss spectrum is shown in Fig. 3. The points represent the observed scattered intensity at a given energy loss W while the line is generated from Eq. (5). The zero energy-loss channel was taken to be at the position of the elastic peak. This, and the energy resolution (FWHM) Δ, were parameters in the fit which were varied until the optimum deconvolution of the spectrum was determined when the difference between the calculated and experimental spectrum was minimized in a least-squares sense.

In the present set of experiments the typical overall energy resolution of the monochromator was ~60 meV (FWHM). This was determined from the fitting program as indicated in Eq. (8). The validity of the fit was tested by direct measurement of both the elastic and a'' peaks and the value from the fit confirmed. In the energy-loss range between 6 and 12.4 eV there are about 150 vibrational sublevels of the ten electronic states of interest. Consequently, the fitting procedure given by Eq. (5) is essential to determine the relative cross sections for each electronic state.

Differences between the calculated spectra and those which were measured experimentally have been discussed by Cartwright *et al.*,[4] who argued that these discrepancies could be due to any deviations of the instrumental profile from the perfect Gaussian shape assumed in the analysis, spurious noise pulses which affected the experimental data, and any breakdown in the Born-Oppenheimer and/or Franck-Condon approximation which would bring into question the validity of the Franck-Condon factors used in the deconvolution procedure.

The computational analysis used in the present study resulted in the determination of the relative contribution of each electronic state to an energy-loss spectrum at a particular incident electron energy and scattering angle. That is, it determined the coefficients $X_{n'}(E,\theta)$. The parameters $X_{n'}(E_0,\theta)$, for a given spectrum, were uniquely determined in the sense that no matter what values were initially chosen for the fit the same final (optimum) values were always determined by the deconvolution procedure. The $X_{n'}(E_0,\theta)$ were then utilized to calculate the ratios $R_{n'}(E_0,\theta)$:

$$R_{n'}(E_0,\theta)=\frac{X_{n'}(E_0,\theta)}{X_{a''\,^1\Sigma_g^+}} \ . \tag{9}$$

The values of $R_{n'}$ determined from the deconvolution were further verified, for a given beam energy and scattering angle, by measuring at least one other energy-loss spectrum, performing the deconvolution, and requiring that the "new" values of $R_{n'}$ were consistent with the original set to better than 10%.

The ratio R_e was determined by scanning the energy loss through the elastic peak, out to 12.4 eV:

$$R_e(E_0,\theta)=\frac{X_{a''\,^1\Sigma_g^+}(E_0,\theta)}{X_{\rm el}(E_0,\theta)} \ . \tag{10}$$

A typical energy-loss spectrum is shown in Fig. 5.

The product of Eqs. (9) and (10) yielded a value for the ratio R_f:

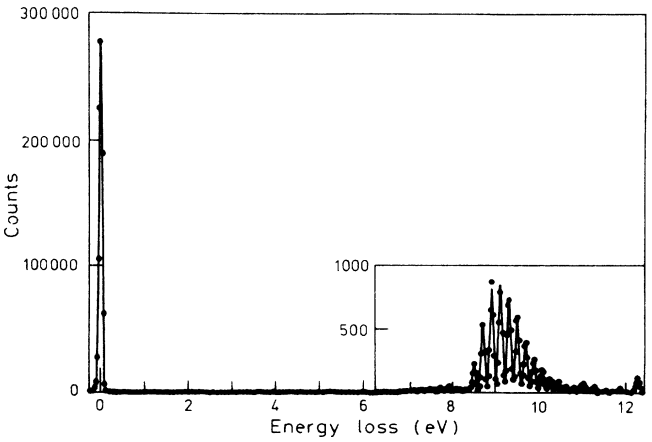

FIG. 5. Energy-loss spectrum in N_2. The electron scattering angle was 20° and the incident electron beam energy was 50 eV. The present data (●) and the fit to this data (——) are shown.

$$R_f=R_{n'}R_e$$

$$\Longrightarrow R_f(E_0,\theta)=\frac{X_{n'}(E_0,\theta)}{X_{\rm el}(E_0,\theta)} \quad \forall n'=1,\ldots,10 \ . \tag{11}$$

Substitution of Eq. (6) into Eq. (11) yields

$$R_f(E_0\theta)=\frac{\sigma_{n'}(E_0,\theta)}{\sigma_{\rm el}(E_0,\theta)} \quad \forall n'=1,2,\ldots,10 \ , \tag{12}$$

where $\sigma_{n'}(E_0,\theta)$ is the differential cross section for the excitation of the n' electronic level and $\sigma_{\rm el}$ is the elastic differential cross section. Thus the desired cross section can be derived from the ratios R_f and the appropriate elastic differential cross section.

B. Normalization of the cross sections

For the present normalization we had a choice between using the absolute elastic cross sections of Srivastava, Chutjian, and Trajmar[35] as reported by Cartwright *et al.*,[4] the renormalized measurements of Srivastava, Chutjian and Trajmar[35] as reported by Trajmar, Register, and Chutjian,[2] or the measurements of Shyn and Carignan.[36] In general, at the energies studied, the absolute values of Shyn and Carignan[36] were somewhat more forward peaked than those reported by either Cartwright *et al.*[4] or Trajmar, Register, and Chutjian.[2] From 60° to 90°, however, all the data are in good agreement. To aid us in our choice of which set of elastic differential cross sections we should use to normalize our data we measured our own set of elastic angular distributions at 15, 17.5, 20, 30, and 50 eV incident electron beam energies and, in each case, over the scattered electron angular range 10°–90°. The procedure used to obtain the elastic N_2 angular distributions was that at each beam energy and every scattering angle the elastic peak was scanned for a preset number initially with the target gas on and then with the target gas off. The gas on and gas off spec-

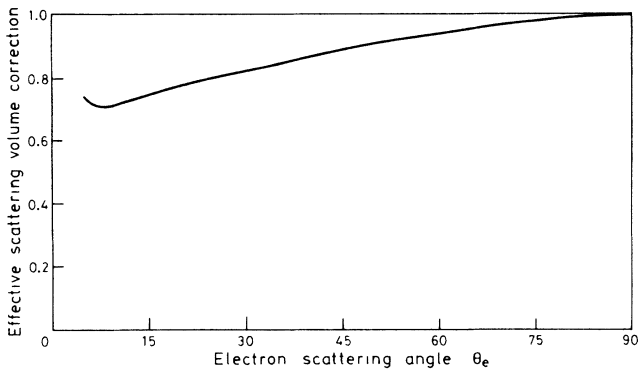

FIG. 6. Derived effective scattering volume correction factor as a function of the electron scattering angle.

tra were then subtracted at each scattering angle to give an angular distribution.

The scattering geometry used in the angular distribution experiments meant that the scattered intensity had to be corrected for the variation in the effective path length as the scattering angle was varied. Brinkmann and Trajmar[37] have calculated correction factors for a number of model scattering geometries including those used in the present experiments. Alternatively the effective path-length correction could be derived by comparing the measured angular distribution with a known differential cross section. Consequently, the angular distribution for elastic scattering of 3 eV electrons from helium was measured and compared with the theoretical predictions of Nesbet[38] at this energy. The derived correction factors at each angle, shown in Fig. 6, are almost identical to those calculated by Brinkmann and Trajmar[37] for a scattering geometry similar to our own.

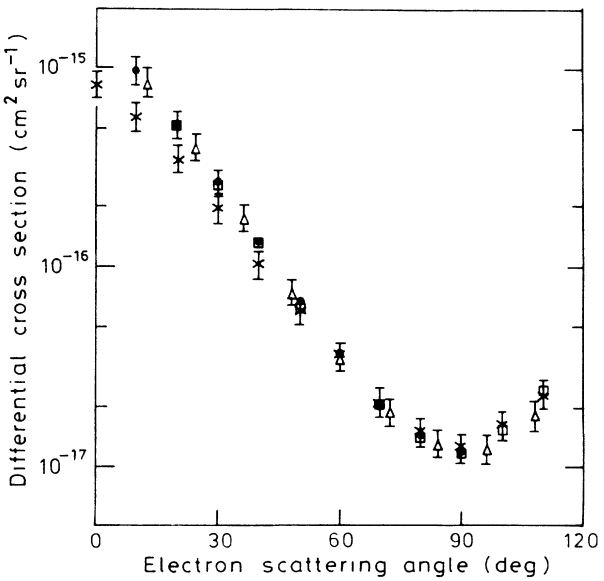

FIG. 7. Elastic differential cross section for electrons of incident beam energy 30 eV. The present data (●) are compared with the earlier work of Shyn and Carignan (Ref. 36) (△), Srivastava, Chutjian, and Trajmar (Ref. 35) (×), and Nickel *et al.* (Ref. 39) (□).

The N_2 elastic angular distributions, at each respective energy studied, were then made absolute by normalizing to a point where both Cartwright *et al.*[4] and Shyn and Carignan[36] agreed in absolute value. In all cases studied the present angular distributions were in excellent agreement with the experiments of Shyn and Carignan.[36] An explicit example of this point for electrons with an incident beam energy $E_0 = 30$ eV is given in Fig. 7. Consequently, the elastic differential cross sections of Shyn and Carignan[36] have been used to normalize our data. At 17.5 eV we have made an interpolation of the elastic cross sections at 15 and 20 eV.

More recently, Nickel *et al.*[39] have measured absolute elastic differential cross sections for N_2 in the energy range 20–100 eV. At each of the energies of mutual interest their[39] data are in excellent agreement with the present results and with the earlier work of Shyn and Carignan.[36]

C. Experimental uncertainties

Chutjian and Cartwright[40] discuss in some detail the sources of error which can be encountered in the measurement, analysis, and normalization procedures for the type of experiments conducted in the present study. The three classes of individual error which can be identified are as follows.

(i) Error in the deconvolution of each feature from nearby features.

(ii) Error in converting at each energy and angle, to an intensity relative to the elastic scattering intensity.

(iii) Error in the elastic differential scattering cross sections.

In the present measurements the ratios $R_f(E_0,\theta)$ were required to be reproducible to better than 10% before they were considered to have been determined. The uncertainties in the elastic differential cross sections of Shyn and Carignan[36] used in the normalization procedure were, in general, of the order 14% across the angular range. Hence the errors in (ii) and (iii) were taken as 10% and 14%, respectively, for the current work. The error in (i) depends on the strength and degree of resolution of the feature in the experimental data. Chutjian and Cartwright[40] divided this deconvolution error into three classes: (a) 10% or less, (b) 10–25%, (c) 26–50%. While the present data (see Figs. 3 and 5) all have good signal-to-noise characteristics and therefore the observed features are clearly defined one must remember that these features contain two or more unresolved vibrational sublevels. Hence while for any given energy-loss spectrum, some of the electronic states would be determined very accurately with a deconvolution error $< 10\%$, others would not be determined so accurately and would have a deconvolution error $\geq 10\%$. We note that for a reasonable χ^2 fit the typical uncertainties in the fitting parameters, as determined by the curvature matrix, are negligible ($\leq 1\%$). This, however, is more a reflection of the

internal self-consistency of the fit rather than a determination of the respective deconvolution errors. There appears to be no generally accepted procedure in the literature to quantify precisely the deconvolution error for a particular electronic state and in the absence of this we have taken the error in (i) to be 10%.

Each of the steps (i), (ii), and (iii) in the process of obtaining differential cross sections are considered to be independent so that the overall error in the absolute differential cross sections is taken as the quadrature sum of errors in (i), (ii), and (iii).

IV. RESULTS AND DISCUSSION

Differential cross section for excitation of the $A\ ^3\Sigma_u^+$, $B\ ^3\Pi_g$, $W\ ^3\Delta_u$, $C\ ^3\Pi_u$, $B'\ ^3\Sigma_u^-$, $a'\ ^1\Sigma_u^-$, $a\ ^1\Pi_g$, $w\ ^1\Delta_u$, $E\ ^3\Sigma_g^+$, and $a''\ ^1\Sigma_g^+$ states in N_2 have been measured. The present work determined these differential cross sections for electrons of incident energy 15, 17.5, 20, 30, and 50 eV, respectively, over the scattered electron angular range 10°–90°. The upper limit of this angular range was restricted to 90° by the physical dimensions of the hemisphere baseplates. This prevented the study of the backward angle behavior of the differential cross sections which in turn limited our ability to deduce integral cross sections for all states other than those which are peaked in the forward direction. Tabulated values of the differential cross sections are given in Tables I–X.

Both the present results and those of Cartwright *et al.*[4] used essentially the same technique to arrive at the differential cross sections. That is, ratios R_f were converted into differential cross sections by multiplying them with the appropriate elastic differential cross section. The elastic differential cross sections used in the present study were, in general, more strongly peaked in the forward direction than those used by Cartwright *et al.*[4] This problem has been corrected to some degree in the renormalized data reported by Trajmar, Register, and Chutjian[2] where, in general, these data improved the agreement with the present results at forward angles.

$A\ ^3\Sigma_u^+$ state (excitation energy = 6.168 eV)

Cross sections for the excitation of the $A\ ^3\Sigma_u^+$ state are given in Table I. The overall agreement between these data and the results of Cartwright *et al.*[4] is poor. At incident energies of 17.5 and 30 eV the renormalized data of Trajmar, Register, and Chutjian[2] are in better agreement with the present results but at the other energies the agreement is still poor. Figure 8 shows the present data at 15 eV where they are compared with the renormalized data of Trajmar, Register, and Chutjian,[2] the data of Cartwright *et al.*,[4] and recent measurement of Zetner and Trajmar.[3] It is clear that there is excellent agreement with the work of Zetner and Trajmar[3] over most of the angular range.

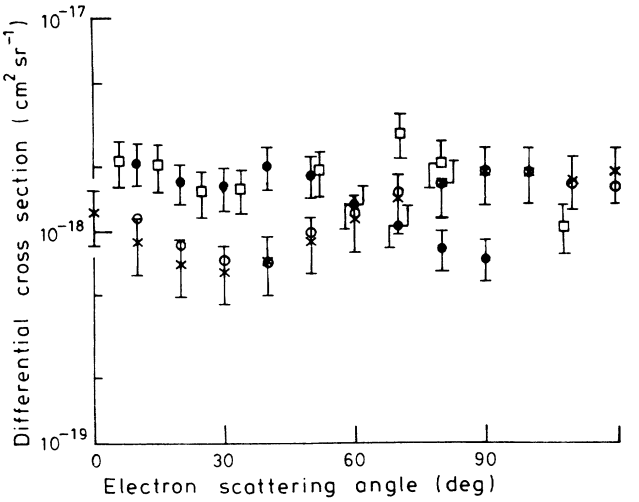

FIG. 8. Differential cross section for the electron-impact excitation of the $A\ ^3\Sigma_u^+$ state by 15-eV electrons. The present data (●) are compared with that derived from Cartwright *et al.* (Ref. 4) (×), Trajmar, Register, and Chutjian (Ref. 2) (○), and Zetner and Trajmar (Ref. 3) (□).

$B\ ^3\Pi_g$ state (excitation energy = 7.353 eV)

Cross sections for the excitation of this state are shown in Table II. There is very poor agreement between the present measurements and all of the earlier results over much of the kinematic range. At 20 eV the agreement is acceptable for $\theta \leq 80°$. In this case, the recent results of Zetner and Trajmar[3] at 15 eV do not resolve the conflict. The sets of data are shown in Fig. 9, from which it can be seen that while both the shape and magnitude of the recent data[3] are in better agreement with the present work,

TABLE I. Differential cross sections (10^{-18} cm^2 sr^{-1}) for electron-impact excitation of the $A\ ^3\Sigma_u^+$ state.

Scattering angle	$\sigma(\theta)$ Incident electron beam energy (E_0) in eV				
θ_e (deg)	15.0	17.5	20.0	30.0	50.0
10	2.097	1.110	0.092	0.416	0.547
20	1.706	1.060	0.138	0.306	0.278
30	1.621	0.949	0.199	0.244	0.179
40	2.025	0.739	0.258	0.152	0.124
50	1.821	0.947	0.265	0.175	0.123
60	1.326	1.304	0.293	0.253	0.110
70	1.083	1.630	0.361	0.275	0.129
80	0.827	1.590	0.268	0.383	0.132
90	0.744	1.703	0.229	0.444	0.109

TABLE II. Differential cross sections (10^{-18} cm^2 sr^{-1}) for electron-impact excitation of the $B\ ^3\Pi_g$ state.

Scattering angle	$\sigma(\theta)$ Incident electron beam energy (E_0) in eV				
θ_e (deg)	15.0	17.5	20.0	30.0	50.0
10	1.526	1.129	0.398	0.312	0.220
20	1.935	2.160	0.507	0.560	0.217
30	2.633	3.285	0.794	0.685	0.208
40	4.049	2.246	0.674	0.525	0.190
50	6.455	2.085	0.464	0.488	0.199
60	5.134	2.495	0.392	0.508	0.182
70	4.270	2.685	0.386	0.537	0.194
80	4.173	3.127	0.369	0.669	0.207
90	5.535	4.126	0.434	0.838	0.230

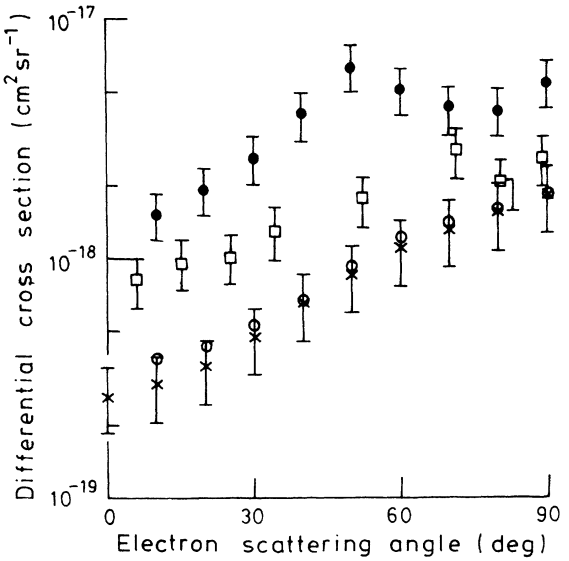

FIG. 9. Differential cross section for the electron-impact excitation of the $B\,^3\Pi_g$ state by 15-eV electrons. The present data (●) are compared with that derived from Cartwright *et al.* (Ref. 4) (×), Trajmar, Register, and Chutjian (Ref. 2) (○), and Zetner and Trajmar (Ref. 3) (□).

the absolute values of the cross sections still differ by a factor of about 2 over the whole angular range.

$W\,^3\Delta_u$ state (excitation energy =7.355 eV)

If we next consider the electron-impact excitation of the $W\,^3\Delta_u$ electronic state then when one compares the present data with that of Cartwright *et al.*[4] and Trajmar, Register, and Chutjian[2] it is found that at both 15 and 17.5 eV there is excellent agreement in terms of the shape of the differential cross sections and in terms of their respective absolute values. With respect to the 15 eV data of Zetner and Trajmar[3] then one observes that the shapes of the two sets of data are also in excellent agreement, although we note that the agreement in terms of the absolute values of the differential cross section is only fair. This is illustrated in Fig. 10, which depicts the 15-eV differential cross section for electron excitation of the $W\,^3\Delta_u$ state. At 20, 30, and 50 eV the shapes of the sets of measurements are found to be in good agreement, although we note that the present data are somewhat smaller in magnitude than those of the previous studies. Tabulated values for the present $W\,^3\Delta_u$ differential cross sections are given in Table III.

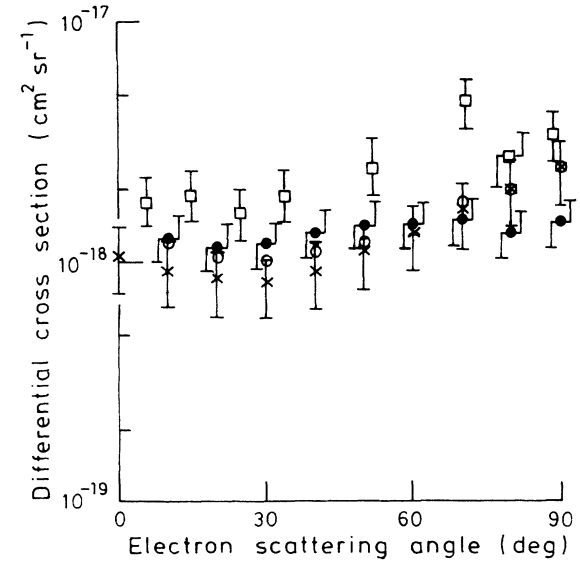

FIG. 10. Differential cross section for the electron-impact excitation of the $W\,^3\Delta_u$ state by 15-eV electrons. The present data (●) are compared with that of Cartwright *et al.*[4] (Ref. 4) (×), Trajmar, Register, and Chutjian (Ref. 2) (○), and Zetner and Trajmar (Ref. 3) (□).

$B'\,^3\Sigma_u^-$ state (excitation energy =8.164 eV)

Differential cross sections for electron-impact excitation of the $B'\,^3\Sigma_u^-$ state are given in Table IV. The present data at both 30 and 50 eV incident electron beam energies are in excellent agreement with the earlier work of Cartwright *et al.*[4] and Trajmar, Register, and Chutjian,[2] across the common angular range of measurement, in terms of the shape and absolute value of the differential cross sections. This is not, however, the case

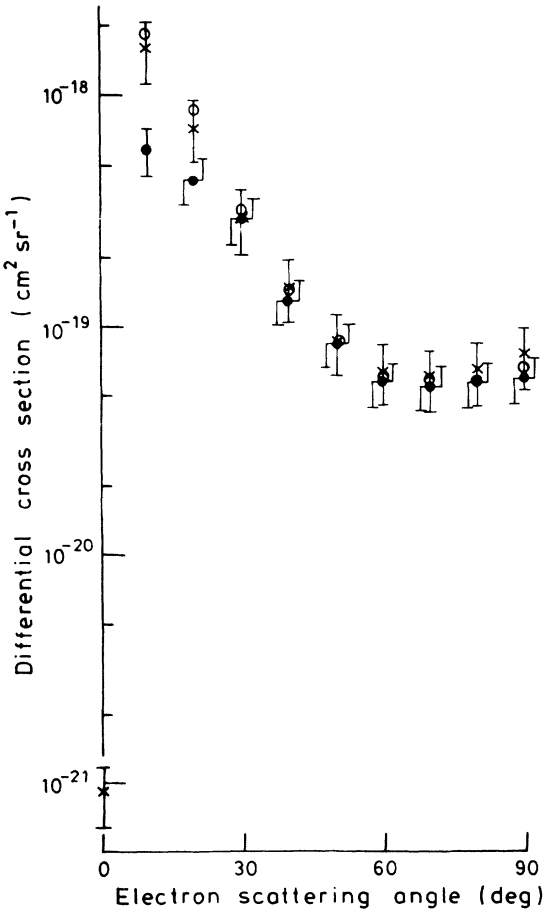

FIG. 11. Differential cross section for the electron-impact excitation of the $a'\,^1\Sigma_u^-$ state by 50-eV electrons. The present data (●) are compared with the earlier studies of Cartwright *et al.* (Ref. 4) (×) and Trajmar, Register, and Chutjian (Ref. 2) (○).

TABLE III. Differential cross sections (10^{-18} cm^2 sr^{-1}) for electron-impact excitation of the $W\,^3\Delta_u$ state.

Scattering angle	$\sigma(\theta)$ Incident electron beam energy (E_0) in eV				
θ_e (deg)	15.0	17.5	20.0	30.0	50.0
10	1.296	0.859	0.440	0.003	0.035
20	1.174	1.384	0.380	0.069	0.036
30	1.211	1.398	0.312	0.102	0.040
40	1.353	1.146	0.265	0.115	0.042
50	1.472	1.192	0.192	0.126	0.044
60	1.465	1.453	0.149	0.138	0.056
70	1.506	1.659	0.165	0.130	0.059
80	1.332	2.116	0.179	0.163	0.065
90	1.490	2.468	0.209	0.208	0.057

at 15, 17.5, and 20 eV where the previous experiments[2,4] underestimate the magnitude of the respective differential cross sections.

$a'\,^1\Sigma_u^-$ state (excitation energy =8.398 eV)

Tabulated values of the differential cross sections for electron-impact excitation of the $a'\,^1\Sigma_u^-$ state are given in Table V. It was found that the present measurements were in very good agreement with the earlier work[2,4] over the scattering angle range of mutual interest and at each of the energies studied. This point can be observed by referring to Fig. 11, which illustrates the 50 eV differential cross section for excitation of the $a'\,^1\Sigma_u^-$ state.

$a\,^1\Pi_g$ state (excitation energy =8.548 eV)

Differential cross sections for the excitation of this state are given in Table VI. At 20, 30, and 50 eV there is excellent agreement between the present results and those of Trajmar, Register, and Chutjian[2] and Cartwright *et al.*[4] over the whole angular range. Figure 12(a) which compares the data at 30 eV, is typical of the agreement at the other energies. At the lower energies, however, the agreement is poor. In particular, at 15 eV the present data are about a factor of 3 higher than those of Cartwright *et al.*[4] The lower values are supported by the renormalized data of Trajmar, Register, and Chutjian[2] while the data of Finn and Doering[41] supports the present data.

TABLE IV. Differential cross sections (10^{-18} cm^2 sr^{-1}) for electron-impact excitation of the $B'\,^3\Sigma_u^-$ state.

Scattering angle	$\sigma(\theta)$ Incident electron beam energy (E_0) in eV				
θ_e (deg)	15.0	17.5	20.0	30.0	50.0
10	1.191	0.686	0.727	0.767	0.589
20	0.793	0.787	0.656	0.479	0.202
30	0.586	0.817	0.596	0.445	0.147
40	0.730	0.829	0.390	0.306	0.075
50	1.619	0.922	0.238	0.238	0.095
60	1.906	1.176	0.210	0.163	0.076
70	1.481	1.285	0.209	0.134	0.066
80	1.360	1.476	0.238	0.153	0.040
90	1.805	1.630	0.358	0.204	0.041

TABLE V. Differential cross sections (10^{-18} cm^2 sr^{-1}) for electron-impact excitation of the $a'\,^1\Sigma_u^-$ state.

Scattering angle	$\sigma(\theta)$ Incident electron beam energy (E_0) in eV				
θ_e (deg)	15.0	17.5	20.0	30.0	50.0
10	0.109	0.067	0.275	0.205	0.587
20	0.213	0.184	0.329	0.323	0.434
30	0.454	0.170	0.387	0.372	0.291
40	0.644	0.150	0.296	0.279	0.130
50	1.236	0.174	0.194	0.186	0.084
60	1.697	0.196	0.114	0.134	0.056
70	1.421	0.181	0.103	0.101	0.054
80	1.040	0.171	0.105	0.108	0.056
90	1.477	0.254	0.127	0.139	0.059

While it is true that Finn and Doering[41] did not account for contributions of vibrational substates from other electronic states which exist in the same energy-loss region as the $a\,^1\Pi_g$ state it should be noted that this effect is compensated for by the fact that they have not included contributions by the $v'=6\rightarrow 10$ vibrational sublevels of the $a\,^1\Pi_g$ state which contain some 25% of the intensity of the electronic transition.[41]

In an attempt to resolve the discrepancy between the measurements we have used our differential cross sections to obtain a total cross section for the excitation of this state. In order to compensate for the restricted angular range of the present data we have fitted our data to a sixth-order polynomial and extrapolated the data to backward angles. The total cross sections are then found by using Simpson's rule to perform the integration. This technique yields a value 4.24×10^{-17} cm^2 for the total cross section at 15 eV of which only 10% was contributed by the extrapolated backward angle data. This cross section is about 20% higher than that measured by Mason and Newell[7] yet the two measurements agree within the combined uncertainties. On the other hand, the total cross section from the data of Cartwright *et al.*[4] at 15 eV does not agree within th combined uncertainties of the data with the Mason and Newell result. Whilst it is true that the Mason and Newell results were normalized at the peak of the cross section at 17 eV, the good agreement with the data of Aarts and deHeer[42] at the higher energies tends to support the larger value of the

TABLE VI. Differential cross sections (10^{-18} cm^2 sr^{-1}) for electron-impact excitation of the $a\,^1\Pi_g$ state.

Scattering angle	$\sigma(\theta)$ Incident electron beam energy (E_0) in eV				
θ_e (deg)	15.0	17.5	20.0	30.0	50.0
10	16.99	31.84	14.04	12.48	22.05
20	13.65	26.58	11.99	9.378	7.866
30	11.34	20.69	7.549	5.872	2.458
40	9.044	13.23	4.168	2.193	0.729
50	6.712	5.307	1.470	1.083	0.427
60	4.177	1.501	0.775	0.639	0.393
70	2.805	0.847	0.608	0.542	0.348
80	2.044	0.672	0.625	0.824	0.304
90	2.288	0.711	0.859	1.058	0.257

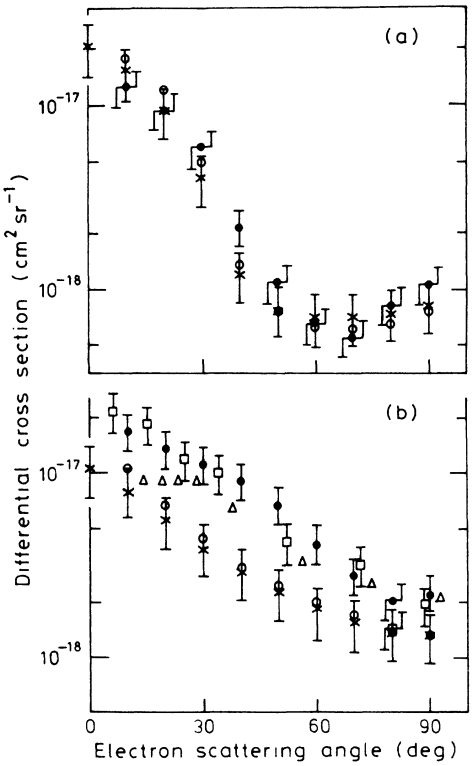

FIG. 12. (a) Differential cross section for the electron-impact excitation of the $a\ ^1\Pi_g$ state by 30-eV electrons. The present data (●) are compared with the earlier studies of Cartwright *et al.* (Ref. 4) (×) and Trajmar, Register, and Chutjian (Ref. 2) (○). (b) Differential cross section for the electron-impact excitation of the $a\ ^1\Pi_g$ state by 15-eV electrons. The present data (●) are compared with the earlier studies of Cartwright *et al.* (Ref. 4) (×), Trajmar, Register, and Chutjian (Ref. 2) (○), Zetner and Trajmar (Ref. 3) (□), and also with Finn and Doering (Ref. 41) (△).

cross section at 15 eV.

The recent 15-eV measurements of Zetner and Trajmar[3] are in excellent agreement with the present data across the entire angular range. This agreement is also reflected by the respective total cross sections as their value[3] of 4.29×10^{-17} cm^2 agrees very well with the present result. All the sets of data are compared in Fig. 12(b) for an incident energy of 15 eV.

TABLE VII. Differential cross sections (10^{-18} cm^2 sr^{-1}) for electron-impact excitation of the $\omega\ ^1\Delta_u$ state.

Scattering angle θ_e (deg)	$\sigma(\theta)$ Incident electron beam energy (E_0) in eV 15.0	17.5	20.0	30.0	50.0
10	1.201	1.447	1.492	0.224	0.327
20	0.903	0.943	0.605	0.141	0.102
30	0.560	0.638	0.236	0.095	0.126
40	0.415	0.273	0.217	0.098	0.058
50	0.211	0.181	0.181	0.081	0.028
60	0.132	0.142	0.166	0.069	0.023
70	0.115	0.134	0.183	0.056	0.023
80	0.169	0.248	0.191	0.059	0.025
90	0.352	0.491	0.206	0.061	0.022

TABLE VIII. Differential cross sections (10^{-18} cm^2 sr^{-1}) for electron-impact excitation of the $C\ ^3\Pi_u$ state.

Scattering angle θ_e (deg)	$\sigma(\theta)$ Incident electron beam energy (E_0) in eV 15.0	17.5	20.0	30.0	50.0
10	5.620	4.230	0.968	0.268	0.167
20	5.737	4.474	1.750	0.415	0.227
30	5.132	3.943	1.615	0.455	0.246
40	5.060	2.610	1.500	0.525	0.167
50	5.063	2.329	1.289	0.499	0.163
60	4.680	2.395	1.139	0.553	0.169
70	4.464	2.593	1.196	0.583	0.180
80	4.218	3.746	1.105	0.614	0.186
90	4.597	3.600	1.076	0.680	0.190

$w\ ^1\Delta_u$ state (excitation energy = 8.889 eV)

Differential cross sections for the excitation of the $w\ ^1\Delta_u$ state are given in Table VII. The present results show a pronounced minimum at about 70° at both 15 and 17.5 eV which was not observed by Cartwright *et al.*[4] There is good agreement at forward angles over the whole energy range. At 50 eV the differential cross sections are in excellent agreement.

$C\ ^3\Pi_u$ state (excitation energy = 11.031 eV)

Differential cross sections for the excitation of this state are given in Table VIII. At 30 and at 50 eV there is

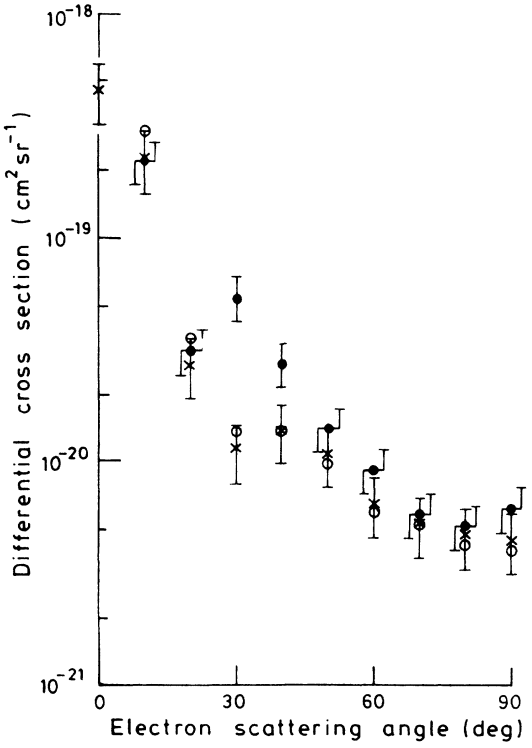

FIG. 13. Differential cross section for the electron-impact excitation of the $E\ ^3\Sigma_g^+$ state by 50-eV electrons. The present data (●) are compared with the earlier studies of Cartwright *et al.* (Ref. 4) (×) and Trajmar, Register, and Chutjian (Ref. 2) (○).

acceptable agreement between the present results and the earlier data. At 15, 17.5, and 20 eV there is serious disagreement at forward angles. This forward angle behavior has important consequences for the total cross section for the excitation of this state at these lower energies. In particular, these results are relevant to the literature on the modeling of gas discharges in N_2. In the absence of backward angle data in the present work we cannot be precise about the total cross section but, as our differential cross sections are everywhere greater than those reported by Cartwright *et al.*, it is clear that our work would support the premise that the total *C*-state cross sections should be greater than those reported by Cartwright *et al.*[4] at 15, 17, and 20 eV. At 17.5 eV we have fitted a sixth-order polynomial to the present results and have used this fit to extrapolate our data to backward angles. The differential cross section was then integrated numerically to yield a total cross section which was 30% higher than that previously reported by Cartwright *et al.*[4] This result is consistent with the observation of Brunger, Teubner, and Buckman[8] that to obtain fair agreement with measured swarm data, Phelps and Pitchford[21,22] were obliged to increase the magnitude of the *C*-state cross section. We note that more recent calculations by Jelenković and Phelps[43] have shown a noticeable improvement in the agreement between the calculated and measured spatial ionization and the $C\ ^3\Pi_u$ excitation coefficients of Tachibana and Phelps[44] when the cross sections for excitation of the $C\ ^3\Pi_u$ state, as compiled by Phelps and Pitchford,[22] were multiplied by 0.67. This is equivalent to increasing the value of the integral cross section of Cartwright *et al.*[5] at 17.5 eV by $\frac{1}{3}$ which is in excellent agreement with the value of the integral cross section derived from the present data.

$E\ ^3\Sigma_g^+$ state (excitation energy = 11.877 eV)

Differential cross sections for electron-impact excitation of the $E\ ^3\Sigma_g^+$ state are given in Table IX. Comparing the present data to that of the earlier studies[2,4] one finds that in most cases there is fairly good agreement in terms of the shape of the differential cross sections. At 50 eV we find that the structure in the cross section, first observed by Cartwright *et al.*,[4] is more pronounced in the present measurement. This point is explicitly shown by Fig. 13. With respect to the magnitudes of the differential cross sections we find that at each of the energies studied the present measurements predict the excitation of the $E\ ^3\Sigma_g^+$ state to be marginally stronger than that found previously.[2,4] In terms of the integral cross sections, however, the present data do tend to support the results of Cartwright *et al.*[5] that, away from threshold where resonance processes dominate,[8] the excitation of the $E\ ^3\Sigma_g^+$ state by electron impact is not particularly strong.

TABLE IX. Differential cross sections (10^{-18} cm^2 sr^{-1}) for electron-impact excitation of the $E\ ^3\Sigma_g^+$ state.

Scattering angle	$\sigma(\theta)$ Incident electron beam energy (E_0) in eV				
θ_e (deg)	15.0	17.5	20.0	30.0	50.0
10	0.027	0.174	0.669	0.416	0.220
20	0.030	0.151	0.450	0.219	0.032
30	0.024	0.129	0.238	0.108	0.055
40	0.029	0.079	0.117	0.089	0.028
50	0.034	0.054	0.059	0.103	0.014
60	0.038	0.025	0.038	0.098	0.009
70	0.030	0.014	0.037	0.069	0.006
80	0.024	0.016	0.038	0.059	0.005
90	0.022	0.022	0.056	0.048	0.006

TABLE X. Differential cross sections (10^{-18} cm^2 sr^{-1}) for electron-impact excitation of the $a''\ ^1\Sigma_g^+$ state.

Scattering angle	$\sigma(\theta)$ Incident electron beam energy (E_0) in eV				
θ_e (deg)	15.0	17.5	20.0	30.0	50.0
10	2.180	1.841	3.835	2.600	1.840
20	0.816	0.959	2.303	0.577	0.237
30	0.444	0.500	1.324	0.473	0.365
40	0.334	0.255	0.758	0.456	0.226
50	0.294	0.189	0.441	0.344	0.176
60	0.261	0.174	0.291	0.277	0.129
70	0.279	0.167	0.254	0.194	0.104
80	0.251	0.179	0.213	0.191	0.087
90	0.283	0.217	0.228	0.189	0.068

$a''\ ^1\Sigma_g^+$ state (excitation energy = 12.253 eV)

Finally, we consider the $a''\ ^1\Sigma_g^+$ state. Here, when we compare the present data to that of both Cartwright *et al.*[4] and Trajmar, Register, and Chutjian,[2] then, at each of the energies studied, it is found that their data are in

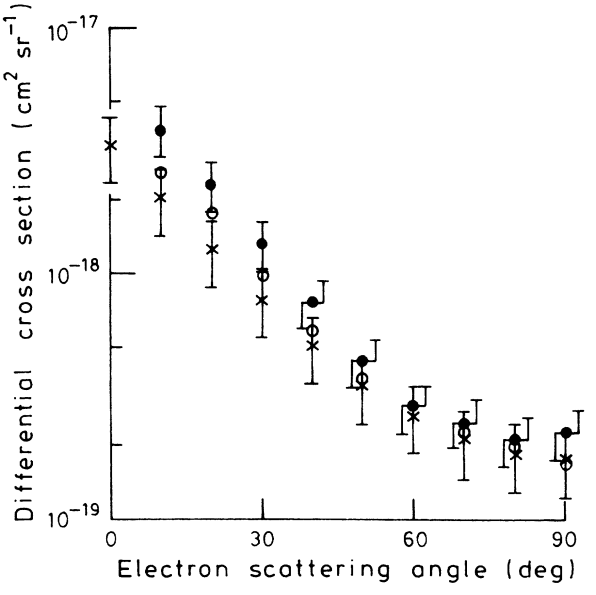

FIG. 14. Differential cross section for the electron-impact excitation of the $a''\ ^1\Sigma_g^+$ state by 20-eV electrons. The present data (●) are compared with the earlier studies of Cartwright *et al.* (Ref. 4) (×) and Trajmar, Register, and Chutjian (Ref. 2) (○).

excellent agreement in terms of the shapes of the differential cross sections. Furthermore, at 15, 17.5, and 50 eV the absolute values of the present results are in very good agreement with those of the earlier studies. At 20 and 30 eV the agreement is still fair, although the earlier data,[4] particularly at the more forward angles, have underestimated the strength of the excitation of this electronic state. The present data at 20 and 30 eV are in good agreement with the renormalized data of Trajmar, Register, and Chutjian[2] which has adequately corrected for the problems, at forward angles, which the data of Cartwright *et al.*[4] suffered from. An excellent example of the good agreement between the two sets of data is provided in Fig. 14 while tabulated values of the present data are given in Table X.

V. CONCLUSIONS

The present results are in fair agreement with the renormalized data of Trajmar, Register, and Chutjian.[2] In general, this agreement improves at the higher energies with the notable exception to this general statement being the set of cross sections for the excitation of the $B\ ^3\Pi_g$ state where the agreement is bad at all angles and at each energy (except 20 eV). The recent results of Zetner and Trajmar[3] agree with the present results with respect to the shape of the differential cross sections for this state at 15 eV but there is poor agreement with the absolute values of these cross sections. However, there is excellent agreement between our data and those of Zetner and Trajmar[3] for the $A\ ^3\Sigma_u^+$ and $a\ ^1\Pi_g$ states, while agreement between the present data and Zetner and Trajmar[3] for the $W\ ^3\Delta_u$ state is fair.

The angular range of our apparatus prevented the study of the backward angle behavior of the differential cross sections. This has limited our ability to deduce total cross sections for states which are not peaked in the forward position. In the case of the $C\ ^3\Pi_u$ state and the $a\ ^1\Pi_g$ state there is a significant difference between the total cross sections of Trajmar, Register, and Chutjian[2] and the present results at 17.5 and 15 eV, respectively. This trend, however, is not sustained for all states and all energies. There is no justification, therefore, in the procedure of manipulating the cross sections of Cartwright *et al.*[4] in order to obtain agreement with the measured swarm parameters. The results given in this paper reinforce the concern of Blevin and co-workers,[45] who note that the manipulation of cross-section sets weakens the predictive power of the simulation technique because of its arbitrary nature.

ACKNOWLEDGMENTS

This research was supported in part by grants from the Australian Research Grants Scheme. M.J.B. acknowledges financial support from the Commonwealth Post Graduate Research Awards Scheme. We would like to thank Mr. R. Scholten for help with some of the numerical aspects of the data analysis technique. We would also like to thank Dr. S. Trajmar for the use of his data prior to publication.

[1] K. Takayanagi, in *Electron-Molecule Collisions and Photoionisation Processes* (Verlag Chemie International, Deerfield Beach, FL, 1983).

[2] S. Trajmar, D. F. Register, and A. Chutjian, Phys. Rep. **97**, 219 (1983).

[3] P. W. Zetner and S. Trajmar, in *Abstracts of the Fifteenth International Conference on the Physics of Electronic and Atomic Collisions, Brighton, 1987,* edited by J. Geddes, H. B. Gilbody, A. E. Kingston, and C. J. Latimer (Queen's University, Belfast, 1987), p. 307; (private communication).

[4] D. C. Cartwright, A. Chutjian, S. Trajmar, and W. Williams, Phys. Rev. A **16**, 1013 (1977).

[5] D. C. Cartwright, S. Trajmar, A. Chutjian, and W. Williams, Phys. Rev. A **16**, 1041 (1977).

[6] J. M. Ajello and D. E. Shemansky, J. Geophys. Res. **90**, 9845 (1985).

[7] N. J. Mason and W. R. Newell, J. Phys. B **20**, 3913 (1987).

[8] M. J. Brunger, P. J. O. Teubner, and S. J. Buckman, Phys. Rev. A **37**, 3570 (1988).

[9] S. Trajmar and D. C. Cartwright, in *Electron-Molecule Interactions and their Applications* (Academic, New York, 1984), p. 156.

[10] L. A. Collins and B. I. Schneider, in *Election-Molecule Scattering and Photoionization,* edited by P. G. Burke and J. B. West (Plenum, New York, 1988), p. 147.

[11] L. A. Collins and B. I. Schneider, in *Electronic and Atomic Collisions, Invited Papers to Fifteenth International Conference on the Physics of Electronic Collisions, Brighton, 1987,* edited by H. B. Gilbody, W. R. Newell, F. H. Read, and A. C. H. Smith (North-Holland, Amsterdam, 1988), p. 57.

[12] V. I. Ochkur, Zh. Eksp. Teor. Fiz. **45**, 346 (1963) [Sov. Phys.—JETP **18**, 503 (1964)].

[13] M. R. H. Rudge, Proc. Phys. Soc. London **87**, 1010 (1966).

[14] B. F. Rozsnyai, J. Chem. Phys. **47**, 4120 (1967).

[15] D. C. Cartwright, Phys. Rev. A **2**, 1331 (1970).

[16] S. Chung and C. C. Lin, Phys. Rev. A **6**, 988 (1972).

[17] W. M. Huo, H. Pritchard, K. Watari, M. A. P. Lima, and V. McKoy, in *Abstracts of the Fifteenth International Conference on the Physics of Electronic and Atomic Collisions, Brighton, 1987,* edited by J. Geddes, H. B. Gilbody, A. E. Kingston, and C. J. Latimer (Queen's University, Belfast, 1987), p. 290.

[18] C. J. Gillan, O. Nagy, P. G. Burke, L. A. Morgan, and C. J. Noble, J. Phys. B **20**, 4585 (1987).

[19] T. Taniguichi, H. Tagashira, and Y. Sakai, J. Phys. D **11**, 1757 (1978).

[20] H. Tagashira, T. Taniguichi, and Y. Sakai, J. Phys. D **13**, 235 (1980).

[21] A. V. Phelps and L. C. Pitchford, Phys. Rev. A **31**, 2932 (1985).

[22] A. V. Phelps and L. C. Pitchford, Joint Institute for Laboratory Astrophysics Information Center Report No. 26, 1985 (unpublished).

[23]E. Harting and F. H. Read, *Electrostatic Lenses* (Elsevier, Amsterdam, 1976).
[24]F. H. Read, J. Comer, R. E. Imhof, J. N. H. Brunt, and E. Harting, J. Electron Spectrosc. Relat. Phenom. **4**, 293 (1974).
[25]R. E. Imhof, A. Adams, and G. C. King, J. Phys. E **9**, 138 (1976).
[26]J. N. H. Brunt, F. H. Read, and G. C. King, J. Phys. E **10**, 134 (1977).
[27]M. J. Brunger, P. J. O. Teubner, A. M. Wiegold, and S. J. Buckman, J. Phys. B **22**, 1443 (1989).
[28]F. Pichou, A. Huetz, G. Joyez, M. Landau, and J. Mazeau, J. Phys. B **8**, L236 (1975).
[29]A. Chutjian, J. Chem. Phys. **61**, 4279 (1974).
[30]S. Trajmar, D. C. Cartwright, and W. Williams, Phys. Rev. A **4**, 1482 (1971).
[31]A. Krupenie and R. H. Lohftus, J. Phys. Chem. Ref. Data. **6**, 113 (1977).
[32]W. Benesch, J. T. Vanderslice, S. G. Tilford, and P. G. Wilkinson, Astrophys. **142**, 236 (1965).
[33]S. Trajmar (private communication).
[34]A. B. Wedding (private communication).
[35]S. K. Srivastava, A. Chutjian, and S. Trajmar, J. Chem. Phys. **64**, 1340 (1976).
[36]T. W. Shyn and G. R. Carignan, Phys. Rev. A **22**, 923 (1980).
[37]R. T. Brinkmann and S. Trajmar, J. Phys. E **14**, 245 (1981).
[38]R. K. Nesbet, Phys. Rev. A **20**, 58 (1979).
[39]J. C. Nickel, C. Mott, I. Kanik, and D. C. McCollum, J. Phys. B **21**, 1867 (1988).
[40]A. Chutjian and D. C. Cartwright, Phys. Rev. A **23**, 2178 (1981).
[41]T. G. Finn and J. P. Doering, J. Chem. Phys. **64**, 4490 (1976).
[42]J. F. M. Aarts and F. J. deHeer, Physica **52**, 45 (1971).
[43]B. M. Jelenković and A. V. Phelps, Phys. Rev. A **36**, 5310 (1987).
[44]K. Tachibana and A. V. Phelps, J. Chem. Phys. **71**, 3544 (1979).
[45]L. J. Kelly, M. J. Brennan, and A. B. Wedding, Aust. J. Phys. (to be published).